Rev.Adv.Mater.Sci. 10 (2005) 249-255

GRAIN STRUCTURE AND TEXTURE DEVELOPMENT DURING ECAP OF TWO HEAT-TREATABLE Al-BASED ALLOYS

Shun Cai Wang[1], Marco J. Starink[1], Nong Gao[1], Cheng Xu[2] and Terence G. Langdon[1,2]

[1]Materials Research Group, School of Engineering Sciences, University of Southampton, Highfield, Southampton SO17 1BJ, United Kingdom
[2]Departments of Aerospace & Mechanical Engineering and Materials Science, University of Southern California, Los Angeles, CA 90089-1453, USA

Received: June 04,2005

Abstract. The microstructures of a spray-cast Al-7034 (Al-Zn-Mg-Cu) alloy and an Al-2024 (Al-Cu-Mg) alloy were studied using electron back-scatter diffraction (EBSD) after processing through equal-channel angular pressing (ECAP). The EBSD results demonstrate there is a relatively rapid increase in the fraction of low-angle boundaries during the initial ECAP passes and a subsequent more gradual increase in the fraction of high-angle grain boundaries in subsequent passes. The crystallographic textures and their rotations during ECAP were analysed through EBSD.

1. INTRODUCTION

Severe plastic deformation (SPD) is a processing technique receiving considerable attention because it has the capability of producing an ultra-fine grain size in the sub-micrometer or nanometer range [1,2]. Equal-channel angular processing (ECAP) is at present one of the most promising techniques having the capability of processing bulk materials sufficiently large for structural applications [3]. In this processing, a sample is pressed through a die in which two channels of equal cross-section intersect at an angle of Φ and an additional angle of ψ defines the arc of curvature at the outer point of intersection of the two channels, as shown in Fig. 1. The influence of the die channel angle was investigated using pure aluminium and channel angles from 90 to 157.5° and it was shown that high-angle grain boundaries (HAGBs) are formed most readily by imposing a very intense plastic strain on the sample in each separate passage through the die when using an angle Φ close to 90° [4].

In this study, the texture, grain orientation and grain structure development of an Al-7034 and an Al-2024 alloy were investigated during ECAP. These alloys are both precipitation-hardening alloys, with the 7xxx alloy able to achieve yield strengths around 700 MPa in an age-hardened condition [5] and the 2024 alloy used mostly for its combination of good fatigue crack growth resistance and good yield strength (typically ~350 MPa in the fatigue-resis-

Corresponding author: M.J.Starink, e-mail: m.j.starink@soton.ac.uk

tant T351 condition). Thus, the present work is an extension to earlier studies which investigated the texture, grain orientation and grain structure development in weaker, non-heat-treatable alloys (see e.g. [6,7]). Electron backscatter diffraction (EBSD) was applied to study the texture/fibre evolution after each processing and to link their relationship between two passages.

2. EXPERIMENTAL MATERIALS AND PROCEDURES

The experiments were conducted on a spray-cast Al-7034 alloy containing, in wt.%, 11.5% Zn, 2.5% Mg, 0.9% Cu, and 0.2% Zr, and on a commercial wrought Al-2024 alloy containing 4.4% Cu, 1.5% Mg, and 0.6% Mn with the balance as Al for both alloys. The Al-7034 alloy was produced in the form of an ingot and extruded into a rod [8]. The Al-2024 alloy was received both in the T351 (solution treated, stretched and subsequently naturally aged) condition and in the form of a fully-annealed condition (annealed at 400 °C) [9]. Only the annealed Al-2024 bars were processed by ECAP. The processing used a solid die with an internal channel having a diameter of 10 mm, with the channel bent through Φ = 90° and with an internal angle (see Fig. 1) of ψ = 20°. Repetitive pressings of the same billets were conducted for both alloys up to a maximum of 8 passes through the ECAP die equivalent to a total imposed strain of ~8 [10]. The Al-7034 billets were pressed at 200 °C and rotated by 90° in the same direction between consecutive passes in the processing route termed B_C [11,12] and the Al-2024 billets were pressed at room temperature using route Bc-C which means they were rotated by 90° after odd-numbered passes and by 180° after even-numbered passes.

To analyse the texture evolution, EBSD was conducted using HKL Channel 5 software on a JEOL JSM-6500F FEG-SEM with a step size of 0.05 μm at 15 kV. The EBSD specimens were electro-polished using a solution of 33% nitric acid in 67% methanol.

3. RESULTS

Al-7034 alloy Fig. 2a shows the grain boundary map of the as-received alloy in which the dark and grey lines represent HAGBs and low angle grain boundaries (LAGBs), respectively. The grains are reasonably equiaxed but inhomogenous in size with an average grain size of ~1.5 μm. Fig. 2b shows a graph of the frequency distribution of the misorientation angles with the superimposed theoretical distribution for an aggregate of randomly-oriented grains. The large difference between the two frequency distributions suggests that the as-received alloy contains strong textures. Moreover, a sharp peak around 55° is noticeable. After a single pass of ECAP, an average grain size of ~1.4 μm was obtained based on the HAGBs and this is quite close to the as-received grain size. At this stage the material contains a relatively large quantity of LAGBs compared to the as-received alloy, as shown by the grey lines in Fig. 2c. The corresponding frequency distribution of the misorientation angles, shown in Fig. 2d, confirms the predominance of LAGBs. The total area fraction of these LAGBs is 68% after the first pass compared to 35% in the as-received alloy. Thus, a single pressing leads to the development of an array of grain boundaries with misorientations below 15°. After 8 ECAP passes the grain size is significantly reduced with an average size of ~0.3 μm (Fig. 2e). The frequency distribution of the misorientation angles in Fig. 2f shows that the fraction of HAGBs increases dramatically with the decrease of grain size.

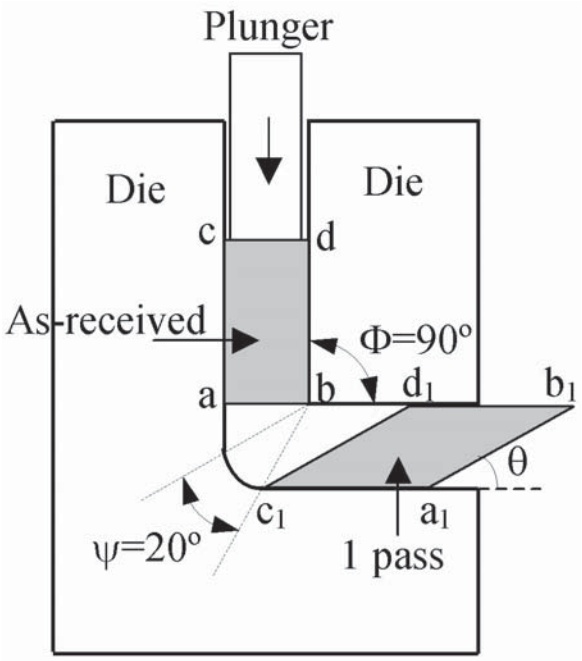

Fig. 1. Schematic illustration of a die used in the present investigation and deformation during one pass processing.

Fig. 3a shows {111} pole figures for the as-received condition. Two distinct rings of <111> and <001> fibre textures exist as illustrated in Fig. 3b.

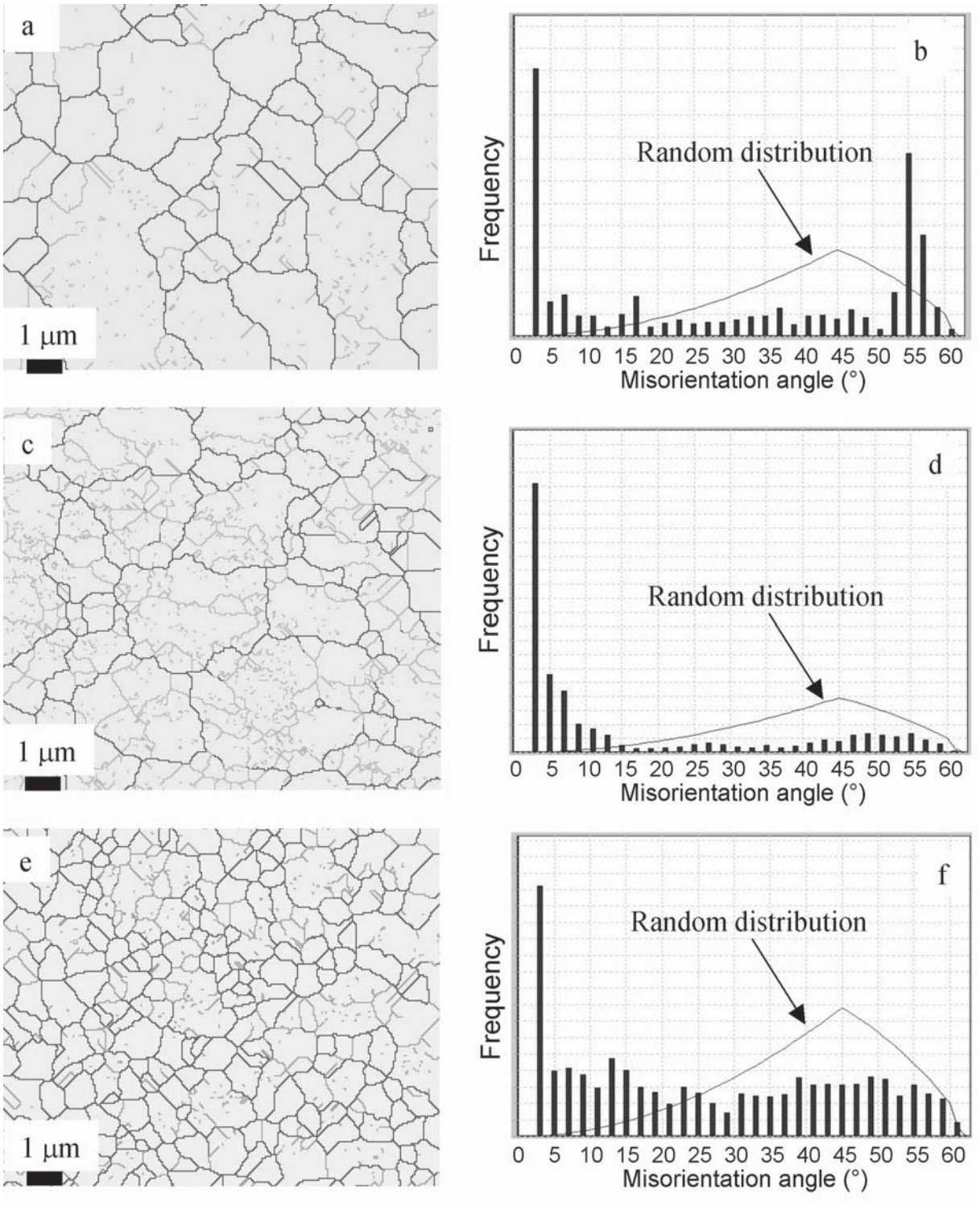

Fig. 2. Grain boundary maps in the Al-7034 alloy (a) in the as-received condition and after (c) 1, (e) 8 passes of ECAP: the dark and grey lines represent misorientation angles >12° and 2-12°, respectively. (b,d,f) are corresponding frequency distributions of misorientation angles in the as-received condition and after 1 and 8 passes of ECAP, respectively.

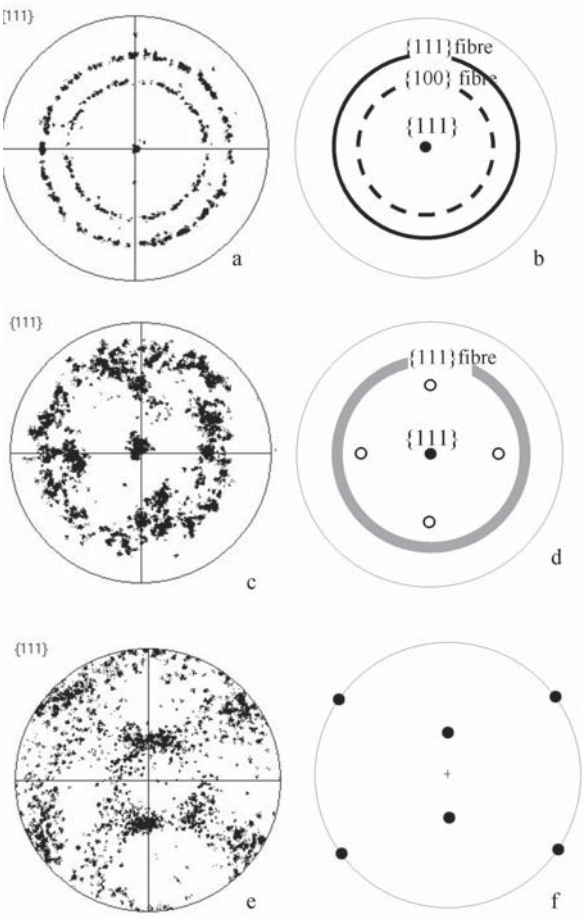

Fig. 3. (a,c,e) {111} pole figures of Al-7034 material in as-received condition and after 1, 8 passes, respectively. (b) Simulated stereographic projection of (a): the bold solid and dashed circles represent <111> and <100> fibre, respectively. (d) Simulated stereographic projection (c): the bold solid circles/spot and open spots represent <111> and {001}<100> cubic textures, respectively. (f) Simulated stereographic projection (e): the spots represent Goss textures {110}<001>.

After the first pass the texture has changed. Viewed at about 40° (i.e. θ = 50°) from the axis of the billet after one pass, the ring of <111> fibre is present in a more diffuse form, the ring of <001> fibre texture has disappeared and four distinct spots have appeared on locations on the <001> fibre texture (Figs. 3c and 3d). After 8 passes, high angle grain boundaries dominate the microstructures and the texture is not as strong as in the as-received material. A weak {110}<001> texture (Goss texture) is present as shown in Figs. 3e-3f.

Al-2024 alloy The Al-2024-T351 alloy is naturally aged and clusters/GPB are the main strengthening mechanism [13,14]. The Vickers hardness was measured as 150 HV [15] and this is too hard to be processed by ECAP at room temperature using the available press. Instead, a fully-annealed alloy with ~60 HV was used for ECAP processing. Low-angle grain boundaries dominate in the T351 condition as shown by the grey lines in Fig. 4a and by the frequency distribution of the misorientation angles in Fig. 4b. The {111} pole figure in Fig. 4c shows typical rolling textures of aluminium. In the annealed condition in Fig. 4d the alloy contained plate-like grains having approximate dimensions of ~500×300 ×10 μm^3 [9]. The frequency distributions of the misorientation angles in Fig. 4e show that the annealed sample has a very low density of LAGBs. The grains are fully recrystallised with the pole {111} pole-figure (Fig. 4f) showing very little evidence for texture.

After 2 passes, the alloy possesses an average grain size of ~2 μm based on the HAGBs and a large quantity of LAGBs (Figs. 4g,h). After these 2 passes some texture has developed (Fig. 4i). These textures are the same as those developed in Figs. 3e and 3f and therefore they are Goss textures. An examination of the microstructures after pressing for a total of 8 passes reveals the presence of arrays of ultrafine and essentially equiaxed grains having average dimensions of ~0.5 μm (Fig. 4j). The frequency distribution of the misorientation angles in Fig. 4k and the {111} pole figure in Fig. 4l show that the grains are essentially randomly oriented. It is therefore confirmed that ECAP processing at room temperature is capable of introducing very substantial grain refinement in the Al-2024 alloy. It is also apparent that the grains in these materials are separated by boundaries having high angles of random misorientation after 8 passes (Figs. 4j-l). Thus, after two passes the amount of LAGBs (Figs. 4g-i) has increased dramatically compared to the as–received sample (Figs. 4d-f). After 8 passes, the grain boundary angle distribution is close to that for a random orientation and HAGBs dominate the microstructure (Figs. 4j-l).

4. DISCUSSION

The misorientation angle distribution for the as-received Al-7034 alloy shows the presence of a peak in the vicinity of ~55° (Fig. 2b). This is due to the existence of two kinds of fibre textures, <001> and <111> (as confirmed in Figs. 3a and 3b), which possess an angle between them of 54.7°. It is interest-

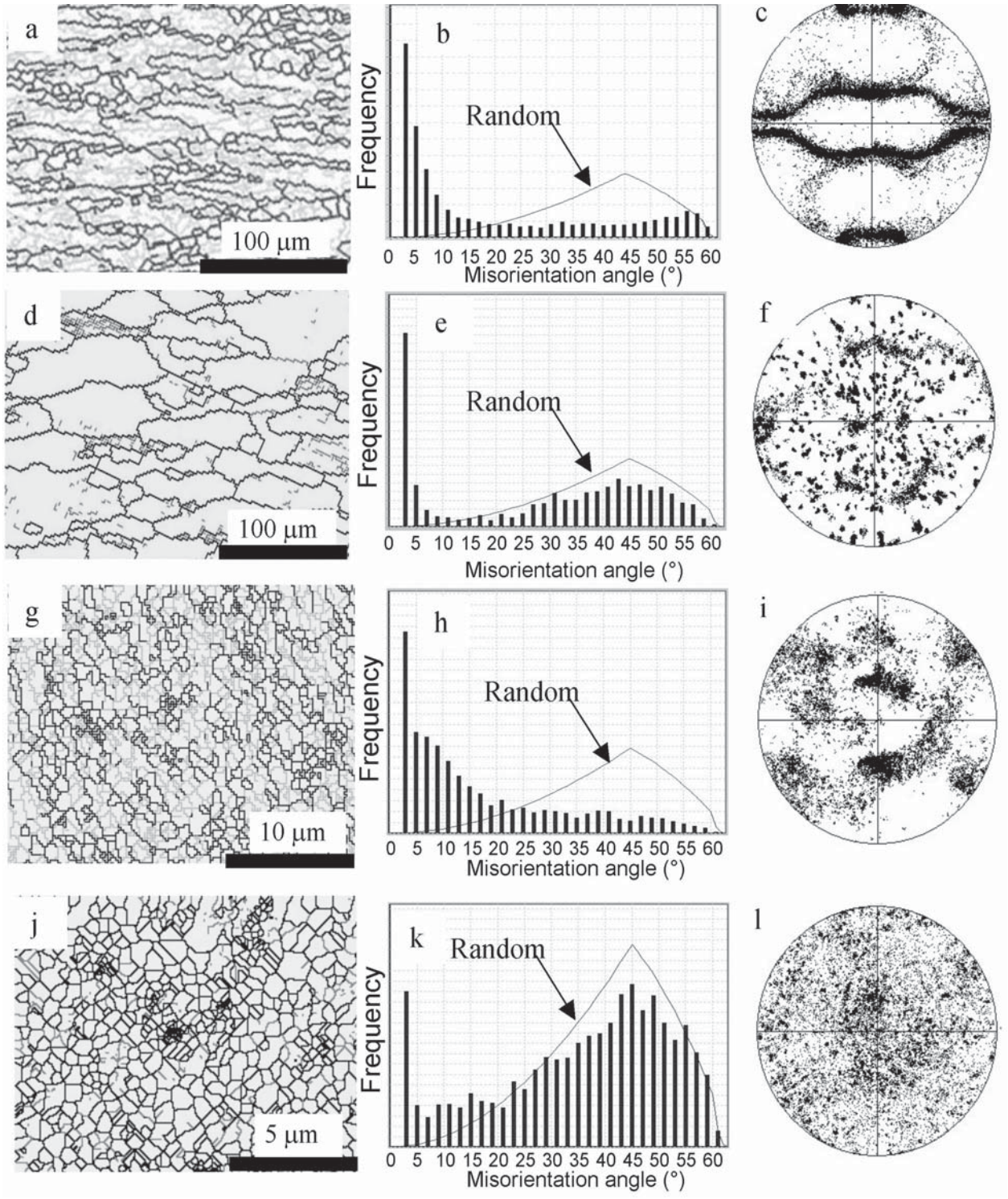

Fig. 4. Grain boundary maps for the 2024 alloy (a) in T351 condition, (d) in the annealed condition and after (g) 2, (j) 8 passes of ECAP: the dark and grey lines represent misorientations >12° and 2-12°, respectively. (b,e,h,k) are the corresponding frequency distributions vs misorientation angles, and (c,f,i,l) are the corresponding {111} pole figures in the T351 condition, in the annealed condition and after 2 and 8 passes of ECAP, respectively.

ing to note that the <111> fibre texture is mostly retained through the first pass of ECAP whereas the <001> fibre texture disappears, indicating that the <111> fibre texture is relatively more stable than the <001> fibre texture during ECAP processing. This is consistent with the general notion that in compression (e.g. simple single-axis compression) the grains tend to rotate such that slip planes become perpendicular to the compression axis (see e.g. [16]). It can be further understood by noting that the <001> fibre is associated with a higher Schmid factor compared to the <111> fibre, which causes a higher activity of slip planes. According to Schmid's law, the Schmid factor, *m*, is

$$m = \cos\lambda \cos\varphi, \quad (1)$$

where λ and φ are the angles of the main tensile axis with a <110> slip direction and {111} slip plane for fcc materials, respectively. Table 1 shows the values of *m* for a total of 12 slip systems for deformation along the axis of the billet. In uniaxial compression, the m value in the [001] direction is as high as 0.41 whilst in [111] it is up to 0.27. Thus, in uniaxial compression the grains of the <111> fibre texture will be more resistant to plastic deformation, and on average they will have fewer active slip systems if activated, so that this texture is more stable.

As the <111> fibre texture is relatively stable after one pass of ECAP, it is possible to find the same plane in the as-received and one pass materials. As shown in Fig. 1, the plane *abcd* shears to $a_1b_1c_1d_1$ in a single pressing through the die. It can be shown that the corresponding shear strain, γ, is given by [10,17]

$$\gamma = \cot(\theta) = 2\cot(\Phi/2 + \psi/2) + \psi/\sin(\Phi/2 + \psi/2) \quad (2)$$

In the present pressing, the ECAP die had angles of $\Phi = 90°$ and $\psi = 20°$, and thus θ is calculated to be 28.7°, which is close to the macroscopic deformation (as indicated in Fig. 1) seen on the sample after one pass. However, as indicated in section 3.1, the actual grain rotation angle to obtain the pole figure in Fig. 3c is $\theta = 50°$. The difference between the theoretical expectation and macroscopic deformation on the one hand and the experimental data for the grain rotation on the other hand means that, at least in the present alloy which possesses strong texture components due to prior conventional extrusion, the shearing in ECAP is more complex than the idealised case. The shearing of individual grains is also likely to depend on the occurrence of local texture components.

A comparison of Figs. 2 and 4 reveals both similarities and marked differences between the two alloys. For both alloys, the first and second passes produce a high fraction of LAGBs and further passes increase the relative fractions of HAGBs. However, these changes appear to be slower for the Al-7034 alloy. After 8 passes of ECAP, the Al-7034 alloy textures still remain whilst the Al-2024 alloy has a nearly random texture. For the 7034 alloy LAGBs seem to be continuously present during the various ECAP passes, whilst for the 2024 alloy the frequency of LAGBs appears to decrease with the number of ECAP passes and approaches a random orientation distribution after 8 passes. This difference is probably caused by a combination of two factors. Firstly, in the Al-7034 alloy a large volume fraction of η particles in a range of sizes is present [8,18]. During processing, dislocation lines bow between the particles until the bowed segments attract and meet leaving Orowan loops around the particles. The loops will further expand and the subsequent dislocations will then pile-up, causing the formation of substantial densities of dislocations and walls of dislocations in each ECAP pass. The density of particles on shear planes in the 2024 alloy is more limited leading to the formation of reduced densities of dislocations and walls of dislocations per pass. Secondly, the Al-7034 alloy contains effective grain boundary pinning particles in the form of the spherical $\beta(Al_3Zr)$ dispersoids [8]. These act to retard the formation of a cellular substructure and inhibit the formation of microshear bands during

Table 1. Schmid factors for 12 slip systems in Al deformed along [111] and [001].

Slip system	[001]	[111]
$(111)[\bar{1}10]$	0	0
$(111)[\bar{1}01]$	0.41	0
$(111)[0\bar{1}1]$	0.41	0
$(\bar{1}11)[110]$	0	0.27
$(\bar{1}11)[101]$	0.41	0.27
$(\bar{1}11)[0\bar{1}1]$	0.41	0
$(1\bar{1}1)[110]$	0	0.27
$(1\bar{1}1)[\bar{1}01]$	0.41	0
$(1\bar{1}1)[011]$	0.41	0.27
$(11\bar{1})[\bar{1}10]$	0	0
$(11\bar{1})[101]$	0.41	0.27
$(11\bar{1})[011]$	0.41	0.27

deformation and thus they essentially hamper the removal of LAGBs. The grain boundary controlling particles in the 2024 alloy are predominantly the Mn-containing T-phase [14] which is less effective than the $\beta(Al_3Zr)$ particles.

5. CONCLUSIONS

1. EBSD analysis of a spray-cast Al-7034 and a commercial Al-2024 alloy shows the first one or two passes of ECAP leads to the formation of LAGBs and there is a relatively rapid increase in the fraction of high-angle boundaries in the subsequent passes leading to a reduction of grain size to ~0.3-0.5 μm. The frequency distributions against misorientation angles also indicate that the textures decrease with increasing numbers of passes in ECAP.
2. During one pass processing of a spray-cast Al-7034 alloy, the <111> fibre is relatively stable whilst the <001> fibre texture evolves to a {001}<100> texture. The different values of the Schmid factors in both [001] and [111] have been calculated to explain the result.
3. After one pass processing of a spray-cast Al-7034 alloy, a shearing angle of $\theta = 50°$ is obtained by means of observation of the unchanged {111} fibre. This is different from a prediction of the shearing angle in a texture-free, monolithic (single phase) alloy.

ACKNOWLEDGEMENTS

This work was funded in part by the INTAS 03-51-3779 project and in part by the National Science Foundation of the United States under Grant No. DMR-0243331.

REFERENCES

[1] R.Z. Valiev, N.A. Krasilnikov and N.K. Tsenev // *Mater. Sci. Eng.* **A137** (1991) 35.
[2] R.Z Valiev, R.K. Islamgaliev and I.V. Alexandrov // *Prog. Mater. Sci.* **45** (2000) 103.
[3] Z. Horita, T. Fujinami and T.G. Langdon // *Mater. Sci. Eng.* **A318** (2001) 34.
[4] K. Nakashima, Z. Horita, M. Nemoto and T. G. Langdon // *Acta Mater.* **46** (1998) 1589.
[5] M.J. Starink and S.C. Wang // *Acta Mater.* **51** (2003) 5131.
[6] A. Gholinia, P. Bate and P.B. Prangnell // *Acta Mater.* **50** (2002) 2121.
[7] P.J. Apps, M. Berta and P.B. Prangnell // *Acta Mater.* **53** (2005) 499.
[8] M.J. Starink, N. Gao, M. Furukawa, Z. Horita, C. Xu and T.G. Langdon // *Rev. Adv. Mater. Sci.* **7** (2004) 1.
[9] S. Lee, M. Furukawa, Z. Horita and T.G. Langdon // *Mater. Sci. Eng.* **A342** (2003) 294.
[10] Y. Iwahashi, J. Wang, Z. Horita, M. Nemoto and T.G. Langdon // *Scripta Mater.* **35** (1996) 143.
[11] M. Furukawa, Y. Iwahashi, Z. Horita, M. Nemoto and T.G. Langdon // *Mater. Sci. Eng.* **A257** (1998) 328.
[12] M.J. Starink, S. C. Wang, N. Gao, H. S. Ubhi, C. Xu and T. G. Langdon // *Mater. Sci. Forum.* **503-504** (2006) 937.
[13] M.J. Starink, N. Gao, L. Davin, J. Yan and A. Cerezo // *Phil. Mag.* **85** (2005) 1395.
[14] S.C. Wang and M.J. Starink // *Inter. Mater. Rev.* **50** (2005), in press.
[15] N. Gao, M.J. Starink, M. Furukawa, Z. Horita, C. Xu and T. G. Langdon // *Proc. of 3rd International Conference on Nanomaterials by Severe Plastic Deformation (NanoSPD3). Mater. Sci. Forum*, in press.
[16] R.E. Smallman and R.J. Bishop, In *Modern Physical Metallurgy & Materials Engineering* (Butterworth Heinemann, Oxford, UK, 1999) 6th edition, p. 233.
[17] M. Furukawa, Z. Horita and T. G. Langdon // *Mater. Sci. Eng.* **A332** (2002) 97.
[18] C. Xu, M. Furukawa, Z. Horita and T.G. Langdon // *Acta Mater.* **53** (2005) 749.